

# CCSD: Cross-Modal Compositional Self-Distillation for Robust Brain Tumor Segmentation with Missing Modalities

Dongqing Xie<sup>1</sup>, Yonghuang Wu<sup>3</sup>, Zisheng Ai<sup>4</sup>, Jun Min<sup>5</sup>, Zhencun Jiang<sup>1</sup>, Shaojin Geng<sup>2</sup>, Lei Wang<sup>12\*</sup>

<sup>1</sup>Shanghai Research Institute for Intelligent Autonomous Systems, Tongji University, Shanghai 200092, China

<sup>2</sup>College of Electronic and Information Engineering, Tongji University, Shanghai 201804, China

<sup>3</sup>College of Biomedical Engineering, Fudan University, Shanghai 201804, China

<sup>4</sup>School of Medicine, Tongji University, Shanghai 200092, China

<sup>5</sup>College of Information Engineering, China Jiliang University, Hangzhou, 310018, China

## Abstract

The accurate segmentation of brain tumors from multi-modal MRI is critical for clinical diagnosis and treatment planning. While integrating complementary information from various MRI sequences is a common practice, the frequent absence of one or more modalities in real-world clinical settings poses a significant challenge, severely compromising the performance and generalizability of deep learning-based segmentation models. To address this challenge, we propose a novel Cross-Modal Compositional Self-Distillation (CCSD) framework that can flexibly handle arbitrary combinations of input modalities. CCSD adopts a shared-specific encoder-decoder architecture and incorporates two self-distillation strategies: (i) a hierarchical modality self-distillation mechanism that transfers knowledge across modality hierarchies to reduce semantic discrepancies, and (ii) a progressive modality combination distillation approach that enhances robustness to missing modalities by simulating gradual modality dropout during training. Extensive experiments on public brain tumor segmentation benchmarks demonstrate that CCSD achieves state-of-the-art performance across various missing-modality scenarios, with strong generalization and stability.

## Introduction

Deep learning has achieved remarkable success in medical image analysis, particularly in brain tumor segmentation tasks. Multi-modal MRI, due to its ability to provide complementary tissue contrast information for precise identification of tumor boundaries and sub-regions, has become the preferred imaging modality for clinical diagnosis (Bakas et al. 2018; Chen et al. 2022). Advanced CNN and transformer architectures by significantly enhance multi-modal MRI segmentation performance through feature fusion and attention mechanisms (Chen et al. 2020; Zhou et al. 2020; Lin and Chen 2024; Tian et al. 2022).

However, in clinical practice, acquiring all four MRI modalities (FLAIR, T1, T1c, T2) is often impossible due to motion, artifacts, or equipment issues. This common modality missing problem severely degrades deep learning performance (Azad et al. 2025; Wu, Wang, and Chen 2024) and limits clinical reliability, as current fusion methods assume full modality availability during training and inference.

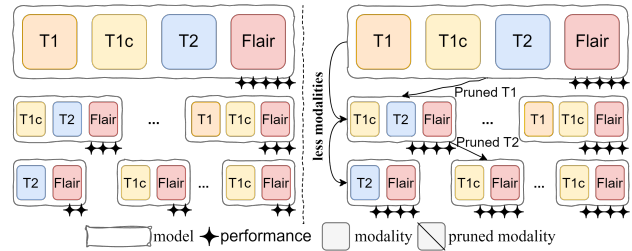


Figure 1: Left: Traditional methods handle modality missing scenarios but lack interaction mechanisms among different modality combinations, resulting in significant performance drops when fewer modalities are available. Right: We propose a cross-modal combination self-distillation approach that introduces two strategies to enable knowledge transfer across hierarchical modality combinations, and simulates modality missing during training to improve robustness and maintain performance under partial modality inputs.

Handling missing modalities in multimodal learning remains a persistent challenge, primarily due to the insufficient flexibility of existing methods in adapting to partial inputs—such as (Chen et al. 2022), which relies on image reconstruction pretraining tasks to accommodate modality absence, or the inadequate cross-modal knowledge transfer, as seen in (Wang et al. 2023), which investigates the lightweight disentanglement and fusion of shared and specific features yet the potential of inter-modal knowledge transfer in enhancing robustness under realistic modality dropout scenarios remains underexplored. Although these issues are widely acknowledged, they have not been adequately addressed by current approaches.

To address these challenges, we propose a novel Cross-Modal Compositional Self-Distillation (CCSD) framework that enhances segmentation performance and robustness under arbitrary modality missing scenarios via a flexible and efficient knowledge transfer mechanism (see Figure 1). Our approach utilizes a Shared-Specific encoder-decoder architecture that effectively disentangles and fuses multi-modal features. Built upon this, we introduce two innovative self-distillation strategies to enhance the model's per-

\*E-mail: wanglei@tongji.edu.cn

formance and robustness in handling multi-modal data: Hierarchical Modality Self-Distillation (HMSD) and Decremental Modality Combination Distillation (DMCD). HMSD bridges semantic gaps across modality hierarchies by transferring knowledge from complete to partial modality sets, enabling richer representation learning. DMCD simulates realistic gradual modality failure by constructing an optimal decrement path, through which sequential distillation progressively strengthens model robustness to partial data availability.

The main contributions of this paper are summarized as follows:

- We proposed a flexible framework to handle arbitrary modality combinations via shared-specific encoders, enabling efficient self-distillation under missing modalities.
- We design a hierarchical modality self-distillation to transfer knowledge from full to partial modalities, reducing conflicts and improving feature consistency.
- We introduce a decremental modality combination distillation strategy to simulate realistic gradual modality failure and employ sequential distillation with dynamic path optimization to simulate progressive modality loss, thereby enhancing robustness.

## Related Work

### Multi-modal Learning

Modern brain tumor segmentation leverages multi-modal MRI (T1, T1c, T2, FLAIR) to capture complementary tumor characteristics. Early CNN-based methods employed dedicated fusion modules for cross-modal integration (Zhang et al. 2021; Zhou et al. 2021; Ding, Yu, and Yang 2021), later enhanced by attention mechanisms that adaptively weight modalities (Lin and Chen 2024; Tian et al. 2022). Recently, Transformer-based (Peiris et al. 2022; Xing et al. 2022; Karimijafarbigloo et al. 2024) and hybrid CNN-Transformer architectures (Wang et al. 2021b; Jia and Shu 2021) have improved long-range modeling and modality interaction. However, these approaches assume complete modality availability, a condition rarely satisfied in clinical practice due to motion artifacts, scanner variability, or protocol mismatches, resulting in significant performance degradation when any modality is absent (Ding, Yu, and Yang 2021; Karimijafarbigloo et al. 2024).

### Missing Modalities

To handle incomplete inputs, existing methods fall into three categories. *Modality augmentation* synthesizes missing images using GANs (Sharma and Hamarneh 2019; Yu et al. 2018) or VAEs (Hamghalam et al. 2021), but often introduces artifacts and performs poorly with single-input scenarios. *Feature space engineering* models inter-modal correlations in latent space through correlation constraints (Ma et al. 2021; Liu et al. 2021), lightweight fusion (Zhang et al. 2024), or feature generation (Kim and Kim 2024). While avoiding explicit synthesis, these methods typically assume consistent missing patterns during training and testing; this limits generalization under rare or unseen combinations (e.g., T1-only). *Architecture engineering* designs

flexible models via masking mechanisms (Qian and Wang 2023), shared representations (Yao et al. 2024), or multi-modal Transformers (Mordacq et al. 2024) that support arbitrary inputs. Though robust in design, many require complex structures or predefined patterns, reducing scalability and impeding knowledge sharing across configurations. Alternative model selection strategies (Wang et al. 2021c; Hu et al. 2020; Li et al. 2023) further trade flexibility for specialization.

Overall, while progress has been made, most methods fail to exploit the shared semantics across different modality subsets, especially under diverse or unobserved missing patterns.

### Knowledge Distillation

Knowledge Distillation (KD) transfers knowledge from a full-modality teacher to students handling partial inputs (Hinton, Vinyals, and Dean 2015), with applications in missing modality tasks (Hu et al. 2020; Wang et al. 2021a; Chen et al. 2021; Azad, Khosravi, and Merhof 2022). However, such co-training schemes incur computational overhead and restrict knowledge flow to fixed teacher-student pairs, ignoring potential synergies across varying input combinations. Self-distillation frameworks (Chen et al. 2022) reduce complexity by sharing parameters within a single network, promoting internal consistency. Yet they still process each modality subset independently, without explicitly aligning representations across combinations.

This insight motivates our key idea that instead of treating different modality combinations in isolation, we can unify them through mutual knowledge exchange within a self-distillation framework that fully accounts for the structural characteristics of modality compositions.

## Method

### Overall Architecture

As shown in Figure 2, we propose a modality-aware encoder-decoder framework built upon a shared-specific disentanglement principle to systematically separate and fuse multi-modal features. The architecture operates as follows: Modality-specific encoders  $E_{\text{spec}}^m$  (one per modality  $m \in \{\text{FLAIR}, \text{T1}, \text{T1c}, \text{T2}\}$ ) first extract domain-adaptive features  $f_{\text{spec}}^m = E_{\text{spec}}^m(x^m)$  that encode unique semantic patterns inherent to each imaging sequence. Concurrently, all modalities are processed through a single shared encoder  $E_{\text{shared}}$  to derive invariant low-level representations  $f_{\text{shared}}^m = E_{\text{shared}}(x^m)$ , establishing a common feature foundation. Crucially, a learnable compositional layer  $C(\cdot)$  then fuses these complementary representations into a discriminative hybrid feature  $f_{\text{fused}}^m = C(f_{\text{shared}}^m, f_{\text{spec}}^m)$ , explicitly modeling both inter-modality commonality and intra-modality specificity. Finally, a shared decoder  $D_{\text{shared}}$  reconstructs the target output from the fused features. This unified design leverages shared representations to ensure cross-modality consistency and modality-specific encoders to preserve specific characteristics, enabling the complementary shared and specific features to further facilitate flexible cross-modality self-distillation as formalized in following sections.

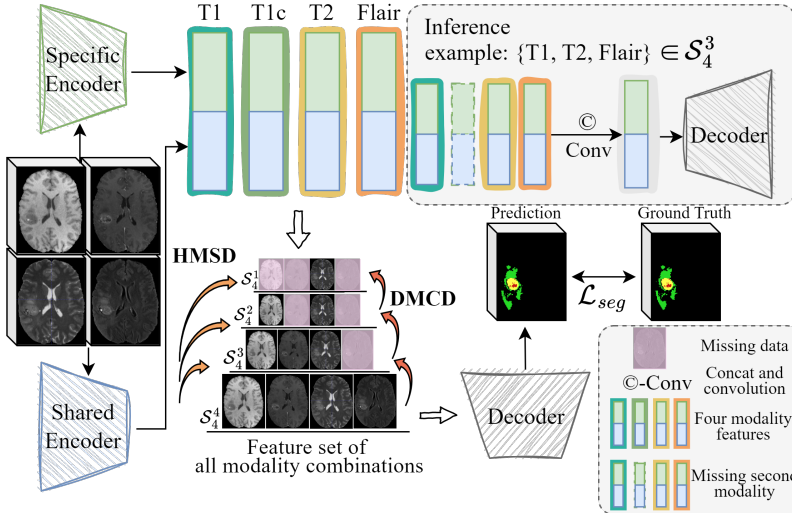


Figure 2: Overview. Left: We employ two encoders to capture both shared and specific features for each modality. For all possible modality combinations, these two types of features are concatenated along both feature and channel dimensions, followed by a lightweight convolutional layer to obtain the fused features for the corresponding modality combination. Based on the fused features, we implement Hierarchical Modality Self-Distillation and Decremental Modality Combination Distillation. The two distillation losses, together with the segmentation loss computed from the decoder using the fused features, are jointly used to optimize the model parameters. During inference, the model can adapt to various scenarios involving missing modalities. Right: Algorithmic illustration of DMCD.  $\mathcal{S}_N^n$ : under ideal conditions with  $N$  modalities, the set of all cases containing only  $n$  modalities.  $\mathcal{S}_i$ : a specific modality combination,  $\tau$ : temperature.

## Handling Full and Missing Modalities

To enable the model to handle input with any combination of modalities, we design a unified forward propagation mechanism. Given a set of  $N$  single modalities  $\mathcal{M} = \{m_1, m_2, \dots, m_N\}$ , the set of all possible non-empty modality combinations is  $\mathcal{S} (|\mathcal{S}| = \sum_{k=1}^N \binom{N}{k} = 2^N - 1)$ . For any input modality subset  $\mathcal{S}_i \subseteq \mathcal{S}$ , our processing pipeline is as follows:

First, for any missing modality  $m_j \notin \mathcal{S}_i$ , we perform a masking operation by setting its corresponding input channel to zero ( $x^{m_j} = 0$ ). Subsequently, the inputs of all modalities (whether present or missing) are passed through their respective encoders.

During the feature fusion stage, for present modalities  $m_j \in \mathcal{S}_i$ , we compute their fused feature  $f_{fused}^{m_j}$ . For the masked missing modalities  $m_j \notin \mathcal{S}_i$ , we directly use their shared feature  $f_{shared}^{m_j}$  as their representation. Finally, we concatenate the features of all modalities to form a unified, high-dimensional feature vector  $Z_{\mathcal{S}_i}$  that represents the current modality combination  $\mathcal{S}_i$ , which is then fed into the decoder.

It is noteworthy that in a single forward pass, we compute and cache the fused features corresponding to all  $2^N - 1$  possible non-empty modality combinations, storing them in a dictionary. This efficient implementation allows us to seamlessly and cost-effectively access the feature representations of any two modality combinations during the training process, facilitating the subsequent KD strategies (see Figure 2).

---

### Algorithm: Decremental Modality Combination Distillation

```

1: Input: Modality combination  $\mathcal{S}_i$ , feature extractor  $F(\cdot)$ 
2: Step1: Criticality Scoring
3: for all  $m_j \in \mathcal{S}_i$  do
4:   Compute  $s(m_j)$ 
5: end for
6: Step2: Decremental Path Construction
7:  $P \leftarrow \{\mathcal{S}_i\}$ 
8: while  $|\mathcal{S}_k| > 1$  do
9:    $m_{remove} \leftarrow \arg \max_{m_j \in \mathcal{S}_k} s(m_j)$ 
10:   $\mathcal{S}_{k-1} \leftarrow \mathcal{S}_k \setminus \{m_{remove}\}$ 
11:  Append  $\mathcal{S}_{k-1}$  to  $P$ 
12: end while
13: Step3: Sequential Distillation
14:  $\mathcal{L}_{DMCD} \leftarrow 0$ 
15: for  $k \leftarrow 2$  to  $|P|$  do
16:    $\mathcal{L}_{DMCD} \leftarrow \mathcal{L}_{DMCD} + D_{KL}(\sigma(Z_{\mathcal{S}_k}/\tau) \parallel \sigma(Z_{\mathcal{S}_{k-1}}/\tau))$ 
17: end for
18: return  $\mathcal{L}_{DMCD}$ 

```

---

## Hierarchical Modality Self-Distillation

In traditional multi-modal distillation methods, knowledge is typically transferred directly from the full modality set to a single modality or a small subset of modalities. However, this direct mapping approach ignores the intermediate hierarchical relationships between different modality subsets, resulting in a knowledge transfer process that is too coarse and abrupt, potentially causing semantic conflicts.

To address this, we introduce the hierarchical modality self-distillation mechanism. This mechanism first randomly selects a hierarchy level  $k$  ( $1 \leq k \leq N - 1$ ) from the  $N$  modalities under the default condition of all modalities being available, and generates all combinations containing exactly  $k$  modalities. For example, when  $N = 4$  and  $k = 3$ , the hierarchical modality set is:

$$\mathcal{S}_4^3 = \{(1, 2, 3), (1, 2, 4), (1, 3, 4), (2, 3, 4)\}. \quad (1)$$

During training, we utilize the full modality set (e.g.,  $(1, 2, 3, 4)$ ) as a powerful teacher network to perform KD in parallel to each student network corresponding to a combination of  $k$  modalities. By enabling modality combinations of different sizes to directly learn the representations of the full modalities, we aim to minimize the distance between all student models and the teacher model in the output space, thereby implicitly enhancing the consistency of feature representations across all modality subsets. The distillation loss is defined as:

$$\mathcal{L}_{HMSD} = \frac{1}{|\mathcal{S}_N^k|} \sum_{\mathcal{S}_i \in \mathcal{S}_N^k} D_{KL}(P_T \parallel P_{\mathcal{S}_i}), \quad (2)$$

where  $P_T$  denotes the output distribution of the teacher model,  $P_{\mathcal{S}_i}$  denotes the output distribution of the student model corresponding to the modality combination  $\mathcal{S}_i$ , and  $D_{\text{KL}}(\cdot)$  is the Kullback–Leibler divergence.

By introducing "modality hierarchy" as an intermediate bridge, this mechanism effectively mitigates the semantic gap problem encountered when distilling directly from the full modalities to combinations with very few modalities, making knowledge transfer smoother and more efficient.

### Decremental Modality Combination Distillation

Although HMSD improves representation quality across multimodal combinations, it treats each missing combination as an independent scenario, failing to exploit structural relationships between related combinations (e.g.,  $\{T1, T2, FLAIR\}$  vs  $\{T1, T2\}$ ) and underrepresenting high-frequency missing patterns. To bridge this gap, we propose **Decremental Modality Combination Distillation**, a training paradigm that deliberately simulates catastrophic data loss scenarios. As illustrated in Algorithm of the Figure 2, DMCD progressively removes the most task-critical modality at each step, starting from the full set  $\mathcal{S}_i$ , until only one modality remains. This systematic degradation forces the model to learn robust compensation strategies for irreversible information loss.

First, a **criticality score**  $s(m_j)$  is defined for each modality  $m_j \in \mathcal{S}_i$  to quantify its contribution to current task performance. A **higher score indicates greater task-criticality** (i.e., higher unique contribution and lower replaceability):

$$s(m_j) = - \sum_{z \neq j} \hat{s}(m_j, m_z) \quad (3)$$

where  $\hat{s}(m_j, m_z)$  is the feature cosine similarity between modalities  $m_j$  and  $m_z$ :

$$\hat{s}(m_j, m_z) = \frac{\langle F(m_j), F(m_z) \rangle}{\|F(m_j)\| \cdot \|F(m_z)\|} \quad (4)$$

Here,  $F(m_j)$  is the feature representation of modality  $m_j$ .

At each step, the modality with the highest criticality score is removed to simulate worst-case data loss:

$$m_{\text{remove}} = \arg \max_{m_j \in \mathcal{S}_i} s(m_j) \quad (5)$$

The modality set is updated  $\mathcal{S}_{i-1} = \mathcal{S}_i \setminus \{m_{\text{remove}}\}$ . This generates a criticality-ordered path  $P$  where each step represents a progressively more severe data failure scenario:

$$P = \{\mathcal{S}_i, \mathcal{S}_{i-1}, \mathcal{S}_{i-2}, \dots, \mathcal{S}_1\} \quad (6)$$

After constructing the path  $P$ , we perform sequential knowledge distillation in reverse order of severity. For adjacent combinations  $(\mathcal{S}_k, \mathcal{S}_{k-1})$  where  $\mathcal{S}_{k-1}$  is missing the most critical modality of  $\mathcal{S}_k$ . We treat the combination  $\mathcal{S}_k$  as the teacher and  $\mathcal{S}_{k-1}$  as the student. The distillation process encourages the student model's feature representation  $Z_{\mathcal{S}_{k-1}}$  to mimic its teacher model's feature representation  $Z_{\mathcal{S}_k}$  as closely as possible. The distillation process trains the student to reconstruct the teacher's representation using

only residual modalities, effectively learning to compensate for the loss of irreplaceable information:

$$\mathcal{L}_{\text{DMCD}} = \sum_{k=2}^{N'} D_{\text{KL}}(\sigma(Z_{\mathcal{S}_k}/\tau) \parallel \sigma(Z_{\mathcal{S}_{k-1}}/\tau)) \quad (7)$$

**Why remove critical modalities?** Conventional approaches avoid removing high-contribution modalities as they are deemed "too important to lose". However, DMCD intentionally induces these worst-case scenarios during training, forcing the model to identify which modalities carry irreplaceable information and learn to reconstruct missing critical information from residual modalities. This directly addresses the limitation of HMSD which only handles random missing patterns, not targeted loss of critical data (see the experimental section below).

## Experiments

**Datasets:** To enable a fair and reproducible comparison with existing methods, this study evaluates the proposed approach on two widely used public benchmarks: BraTS 2018 and BraTS 2020. The datasets contain 285 and 369 training cases, respectively, all of which are publicly available with expert-annotated ground truth labels. Following the consistent data partitioning protocol (Chen et al. 2022), we split the BraTS 2018 dataset into 199 training, 29 validation, and 57 test cases, and the BraTS 2020 dataset into 219 training, 50 validation, and 100 test cases. The input consists of four MRI modalities have undergone standardized pre-processing including skull-stripping, spatial alignment, and isotropic resampling to  $1 \text{ mm}^3$  resolution. Evaluation is performed on three clinically significant tumor subregions: the whole tumor (WT), tumor core (TC), and enhancing tumor (ET), with performance quantified using the Dice Similarity Coefficient (Dice). Final results are reported on the held-out test set. This experimental setup aligns with recent state-of-the-art methods, ensuring a rigorous and objective evaluation under a unified benchmark.

**Implementation:** We adopt the same backbone network as ShaSpec (Wang et al. 2023), which is based on a 3D U-Net architecture. The encoder consists of a shared feature encoder and modality-specific feature encoders, with feature fusion taking place at the early stages of the decoder. The model is optimized using the Adam optimizer with an initial learning rate of  $10^{-2}$ , which is decayed using a cosine annealing schedule. Training is conducted for 100 epochs with a batch size of 12. Data augmentation, including random rotations and flips, is applied to enhance generalization. At inference, the model is evaluated under various missing modality scenarios. Experiments are performed on an NVIDIA A100 GPU. The segmentation performance is evaluated using the Dice score.

## Results

Table 1 and Table 2 compare the performance of our framework on the BraTS 2018 and BraTS 2020 datasets, respectively. For BraTS 2018, we reference (Wang et al. 2023)

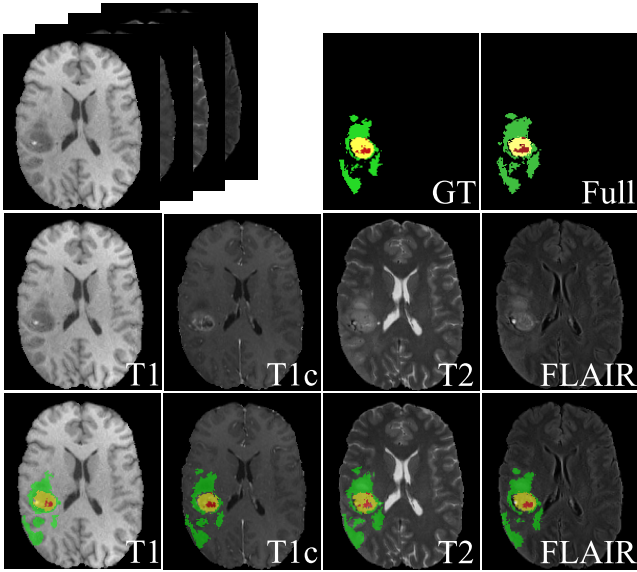


Figure 3: Visualization. Green: edema; yellow: enhancing tumor; and red: necrotic and non-enhancing tumor core. GT: Ground Truth.

and compare against the performance of four recent state-of-the-art methods for brain tumor segmentation with missing modalities: mmFm (Zhang et al. 2022), ShaSpec (Wang et al. 2023), M3AE (Chen et al. 2022), and MIFPN (Diao et al. 2025). For BraTS 2020, we reference the baseline from (Chen et al. 2022) and compare against the following four methods: SMU-Net (Azad, Khosravi, and Merhof 2022), ShaSpec (Wang et al. 2023), M3AE (Chen et al. 2022), and MIFPN (Diao et al. 2025).

Table 1 showcases the performance comparison between our method and four recent state-of-the-art methods for missing modality brain tumor segmentation on the BraTS 2018 dataset. In terms of overall average performance, our method achieves the best results across all three segmentation regions: 62.70% for ET, 78.23% for TC, and 86.47% for WT, representing improvements of 1.93%, 0.3%, and 0.65% over the second-best method, respectively. Figure 3 shows example segmentation results by our method.

In single-modality scenarios, our method performs best in most cases, particularly achieving 90.40% for WT segmentation with Modality 1, significantly outperforming other methods. Our method also demonstrates stable advantages in other modality combination scenarios. More intuitive results are presented in Figure 4.

Table 2 presents the average performance comparison between our method and four competing methods on the BraTS 2020 dataset. The results indicate that our method achieves significant performance improvements across all segmentation regions: 87.21% for WT, an improvement of 0.31% over the best competitor M3AE; 82.54% for TC, an improvement of 3.44%; and 65.93% for ET, an improvement of 4.23%. The overall average performance reaches 78.56%, which is a 2.66% improvement over the second-best method M3AE. This significant enhancement validates the effective-

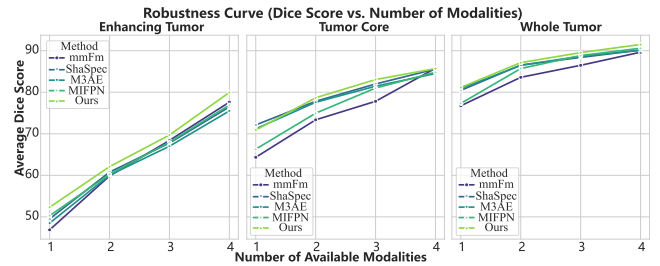


Figure 4: Comparison of average Dice scores across varying numbers of modalities.

ness and robustness of our proposed method.

### Ablation Study

To validate the effectiveness of each key component in our proposed framework, we conducted detailed ablation studies on the BraTS 2018 dataset. Table 3 shows the performance under different combinations of components, where K1 and K2 represent the HMSD and DMCD in our framework, respectively.

When the K1 component is removed, the average performance drops to 75.03%, a decrease of 0.76% compared to the full model, with a slight performance drop observed in ET segmentation. The K2 component contributes more noticeably to the ET segmentation task; its removal causes ET performance to drop from 62.70% to 61.34%, a decrease of 1.36 percentage points. When both K1 and K2 are removed, the model performance further drops to 73.71%, indicating that both components positively contribute to the model’s performance and exhibit a certain degree of synergistic effect.

### Feature Selection for Distillation

To validate the effectiveness of feature selection within our proposed HMSD and DMCD mechanisms, and to investigate the core question of “which features are most suitable for knowledge transfer between modalities,” we designed comprehensive ablation experiments. This section systematically compares the impact of different feature selection strategies on the model’s final performance.

In our model design, specific features  $f_{spec}^m$  and shared features  $f_{shared}^m$  are extracted for each modality, which are then concatenated to form the fused modality feature  $f_{fused}^m$ . To explore which type of feature is more suitable for inter-modal knowledge transfer, we designed the following experiment: we implemented our two proposed distillation strategies (HMSD and DMCD) using  $f_{spec}^m$ ,  $f_{shared}^m$ , and  $f_{fused}^m$  separately. We report the experimental results for using different feature types with different distillation schemes.

As shown in Table 4, the distillation mechanism can effectively address the missing modality problem, but the choice of features leads to differences in performance. The strategy using only specific features  $f_{spec}^m$  for distillation yields the smallest performance gain. This aligns with our theoretical analysis:  $f_{spec}^m$  is highly modality-specific. When a modality is missing, its corresponding specific features are

Table 1: Results on BraTS 2018. Modalities 1-4 denote FLAIR, T1, T1c, and T2, respectively. Results for M3AE\* is taken from (Chen et al. 2022). Metric: Dice score.

Modalities	Enhancing Tumor					Tumor Core					Whole Tumor				
	mmFm	ShaSpec	M3AE*	MIFPN	Ours	mmFm	ShaSpec	M3AE*	MIFPN	Ours	mmFm	ShaSpec	M3AE*	MIFPN	Ours
1	39.33	37.79	35.60	42.28	<b>45.48</b>	61.21	69.26	66.40	62.64	<b>70.89</b>	86.10	89.65	88.70	86.79	<b>90.40</b>
2	32.53	38.43	37.10	40.46	<b>42.82</b>	56.55	<b>66.49</b>	66.10	57.01	65.20	67.52	73.66	<b>74.40</b>	67.75	74.17
3	72.60	<b>74.27</b>	73.70	72.87	74.22	75.41	81.85	<b>82.90</b>	78.86	78.05	72.22	74.35	<b>75.80</b>	73.09	75.52
4	43.05	<b>47.62</b>	47.60	45.49	46.76	64.20	<b>70.90</b>	69.40	66.69	69.43	81.15	84.15	<b>84.80</b>	81.63	84.54
12	42.96	43.85	41.20	44.55	<b>45.58</b>	65.91	72.76	70.80	67.23	<b>73.60</b>	87.06	88.36	89.00	<b>89.85</b>	88.93
13	75.07	76.18	75.00	74.40	<b>76.84</b>	77.88	84.11	<b>84.40</b>	78.13	84.31	87.30	90.33	89.70	89.72	<b>90.46</b>
14	47.52	44.66	45.40	47.09	<b>48.81</b>	69.75	71.72	70.90	70.99	<b>73.17</b>	87.59	90.14	89.90	89.49	<b>92.04</b>
23	74.04	74.53	74.70	74.28	<b>77.01</b>	78.59	82.87	83.40	79.89	<b>84.02</b>	74.42	77.51	77.20	77.03	<b>78.63</b>
24	44.99	<b>48.90</b>	48.70	45.68	47.39	69.42	72.05	71.80	<b>72.34</b>	72.15	82.20	<b>87.31</b>	86.70	84.61	86.47
34	74.51	76.52	75.30	75.65	<b>76.88</b>	78.61	83.44	84.20	81.16	<b>84.79</b>	82.99	85.59	<b>86.30</b>	83.55	86.23
123	75.47	75.87	74.00	76.41	<b>77.63</b>	79.80	84.08	84.10	83.35	<b>85.28</b>	87.33	89.02	88.90	<b>90.01</b>	89.20
124	<b>47.70</b>	44.66	44.80	45.33	47.30	71.52	73.38	72.70	74.41	<b>74.64</b>	87.75	89.46	89.90	89.37	<b>90.24</b>
134	75.67	74.83	73.80	74.93	<b>76.73</b>	79.55	85.69	84.60	83.03	<b>86.86</b>	88.14	89.76	90.20	90.56	<b>90.91</b>
234	74.75	75.74	75.40	75.28	<b>77.14</b>	80.39	84.79	84.40	83.24	<b>85.42</b>	82.71	85.30	85.70	85.40	<b>87.82</b>
1234	77.61	76.47	75.50	76.92	<b>79.95</b>	85.78	85.58	84.50	84.82	<b>85.70</b>	89.64	90.15	90.10	90.59	<b>91.50</b>
Avg.	59.85	60.69	59.85	60.77	<b>62.70</b>	72.97	77.93	77.37	74.63	<b>78.23</b>	82.94	85.65	85.82	84.63	<b>86.47</b>

Table 2: Results on BraTS 2020. Results for SMU-Net\* and M3AE\* are from (Chen et al. 2022). Metric: Dice Score.

Method	SMU-Net*	ShaSpec	M3AE*	MIFPN	Ours
WT	85.30	86.27	86.90	85.48	<b>87.21</b>
TC	77.70	78.53	79.10	78.00	<b>82.54</b>
ET	59.70	59.91	61.70	60.22	<b>65.93</b>
Avg.	74.23	74.90	75.90	74.57	<b>78.56</b>

Table 3: Ablation Study. The experiments were conducted on BraTS 2018. K1 and K2 represent HMSD and DMCD, respectively. Metric: Dice Score.

K1	K2	Whole	Core	Enhancing	Mean
✗		84.68	76.79	61.34	74.27
✗		85.26	77.48	62.36	75.03
✗	✗	85.03	74.61	61.48	73.71
✓	✓	<b>86.44</b>	<b>78.23</b>	<b>62.70</b>	<b>75.79</b>

absent, making knowledge transfer based on them unstable and poorly generalizable. The strategy using only shared features  $f_{shared}^m$  performs better than using specific features. This suggests that the common, invariant representations learned from all modalities serve as a very robust carrier of knowledge, providing reliable and highly generalizable supervisory signals when modalities are missing. The fused features contain the richest information. The strategy using only  $f_{fused}^m$  performs better than the previous two, as it incorporates both shared and specific information, providing the student model with soft targets closest to the final decision.

### Path Construction Strategy Analysis

A critical design choice within our DMCD framework lies in the strategy for constructing the decremental path, which sequence governing the order of modality removal. To rigorously validate the effectiveness of our proposed criticality-based removal strategy, whereby the most critical (highest-scoring) modality is removed at each step, we conducted a comprehensive ablation study comparing it against two

Table 4: Ablation study on the types of features used for distillation: Shared, Specific, and Fusion. Experiments are performed on the BraTS 2018 dataset. Dist.Type: Feature type used in distillation. Metric: Dice Score.

Dist.Type	HMSD	DMCD	Whole	Core	Enhancing	Mean
Shared	✓		82.71	75.28	59.89	72.63
		✓	83.06	75.84	59.32	72.74
	✓	✓	83.75	76.41	60.43	73.53
Specific	✓		80.58	72.19	56.58	69.78
		✓	81.57	72.80	58.13	70.83
	✓	✓	80.17	71.04	56.50	69.24
Fusion	✓		84.68	76.79	61.34	74.27
		✓	85.26	77.48	62.36	75.03
	✓	✓	<b>86.44</b>	<b>78.23</b>	<b>62.70</b>	<b>75.79</b>

alternative approaches. The first alternative, termed Min-Criticality, reverses our logic by prioritizing the removal of the least critical modality first, thereby presenting the model with a progressively more difficult but initially gentler learning trajectory. The second alternative, a Random-Path strategy, severs modality connections in a stochastic order.

We implement all three path construction strategies within the same DMCD framework, keeping all other components identical. The experiment is conducted on the BraTS 2018 dataset. For each strategy, we start with the full modality combination, and then construct a decremental path by iteratively removing one modality according to the respective strategy. Finally, we perform sequential knowledge distillation along the constructed path and evaluate the final model's performance on the test set. For concise, we selected the Flair, T1, and T1c combination for presentation in the Table 5.

Table 5 presents the comparative performance of the three path construction strategies under different evaluation conditions. The proposed DMCD (argmax) achieves the best performance across all evaluation scenarios, with an average Dice of 74.68 compared to 74.17 for Random-Path and 73.68 for Min-Criticality.

These results collectively validate our hypothesis that deliberately constructing paths by removing the most critical modalities first creates more effective training scenar-

Table 5: Results on BraTS 2018. Modalities 1-4 denote FLAIR, T1, T1c, and T2, respectively. Random and Min-C correspond to the Random-Path and Min-Criticality strategy, respectively. Metric: Dice score.

Modalities	Enhancing Tumor			Tumor Core			Whole Tumor		
	Random	Min-C	Default	Random	Min-C	Default	Random	Min-C	Default
1	44.18	43.35	<b>45.48</b>	70.33	69.62	<b>70.89</b>	89.64	88.71	<b>90.40</b>
2	42.94	41.67	<b>42.82</b>	64.62	63.35	<b>65.20</b>	73.95	73.46	<b>74.17</b>
3	73.23	73.42	<b>74.22</b>	77.30	77.06	<b>78.05</b>	75.25	74.84	<b>75.52</b>
12	45.29	43.39	<b>45.58</b>	<b>73.83</b>	72.28	73.60	88.39	88.71	<b>88.93</b>
13	76.17	75.49	<b>76.84</b>	83.21	83.52	<b>84.31</b>	89.77	89.50	<b>90.46</b>
23	76.98	76.48	<b>77.01</b>	83.33	83.03	<b>84.02</b>	78.48	78.53	<b>78.63</b>
123	77.10	77.53	<b>77.63</b>	84.75	84.95	<b>85.28</b>	88.93	88.42	<b>89.20</b>
Avg.	62.27	61.62	<b>62.80</b>	76.77	76.26	<b>77.34</b>	83.49	83.17	<b>83.90</b>

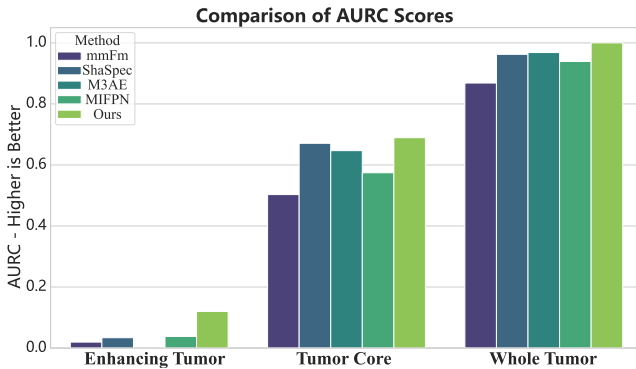


Figure 5: Comparison of AURC scores among our method and four baseline methods on the three segmentation tasks: ET, TC, and WT. AURC evaluates the overall performance and robustness of a model under varying degrees of modality missing by computing the area under the curve of average Dice scores with respect to the number of available modalities. A higher AURC indicates better stability and performance, especially when modalities are missing.

ios for knowledge distillation. The DMCD approach forces the model to learn how to compensate for the loss of irreplaceable information, resulting in better generalization when faced with real-world modality missing scenarios. In contrast, Min-Criticality focuses on easier cases where redundant information is lost, providing less valuable learning signals, while Random-Path lacks the systematic approach needed to build robust multimodal representations.

This experiment provides strong evidence that the specific ordering of modality removal is crucial to the success of decremental distillation, and our criticality-based strategy offers a principled approach to constructing optimal decremental paths for multimodal learning.

## Qualitative Results

To more comprehensively evaluate the overall performance and stability of the model under varying degrees of modality missing scenarios, we introduce the Area Under the Robustness Curve (AURC) as a key quantitative evaluation metric. While the traditional Dice score can show the model’s performance under specific modality combinations, it is diffi-

cult to measure its overall robustness when facing gradually reducing information.

The calculation process of the AURC metric is as follows. First, we group all 15 modality combinations based on the number of available modalities. Second, we calculate the average Dice score for all test cases within each group, resulting in four key performance points. Finally, we plot the “Robustness Curve” with the number of available modalities on the x-axis and the corresponding average Dice score on the y-axis. The AURC is the area under this curve. A higher AURC value indicates that the model’s robustness curve is positioned higher overall, signifying that the model maintains superior comprehensive performance both when information is sufficient and when it is severely lacking.

Figure 5 shows the comparison of AURC scores between our method and the other four methods on the three segmentation tasks: ET, TC, and WT. It can be clearly observed from the figure that our proposed method achieves the highest AURC values across all three tasks. It not only performs excellently when all four modalities are available but, more importantly, its performance declines more gradually when facing the challenge of one or more missing modalities, consistently maintaining a performance advantage over other methods. The consistently leading AURC values fully validate the effectiveness and stability of our framework in handling incomplete multi-modal data, which is of great significance for practical clinical applications.

## Conclusion

In this paper, we tackle the challenge of handling missing modalities in multi-modal brain tumor segmentation by building upon the shared-specific encoder-decoder architecture, which effectively disentangles modality-invariant and modality-specific features. Our primary contribution lies in enhancing this framework with two novel self-distillation strategies: HMSD, which facilitates knowledge transfer from full modality sets to subsets across hierarchy levels, and DMCD, which simulates progressive modality failure scenarios to boost robustness against information loss. This integrated approach elegantly handles arbitrary input modality combinations without requiring architectural changes during inference.

Our work presents a knowledge-oriented solution to the missing modality problem, with significant potential for reli-

able application in clinical settings where incomplete data is prevalent. For future research, we plan to explore advanced feature fusion mechanisms and extend our proposed distillation paradigm to other multi-modal medical image analysis tasks, further enhancing the utility of this approach in diverse clinical contexts.

## References

Azad, R.; Dehghanmanshadi, M.; Khosravi, N.; Cohen-Adad, J.; and Merhof, D. 2025. Addressing missing modality challenges in MRI images: A comprehensive review. *Computational Visual Media*, 11(2): 241–268.

Azad, R.; Khosravi, N.; and Merhof, D. 2022. SMU-Net: Style matching U-Net for brain tumor segmentation with missing modalities. In *International Conference on Medical Imaging with Deep Learning*, 48–62. PMLR.

Bakas, S.; Reyes, M.; Jakab, A.; Bauer, S.; Rempfler, M.; Crimi, A.; Shinohara, R. T.; Berger, C.; Ha, S. M.; Rozycki, M.; et al. 2018. Identifying the best machine learning algorithms for brain tumor segmentation, progression assessment, and overall survival prediction in the BRATS challenge. *arXiv preprint arXiv:1811.02629*.

Chen, C.; Dou, Q.; Jin, Y.; Liu, Q.; and Heng, P. A. 2021. Learning with privileged multimodal knowledge for unimodal segmentation. *IEEE transactions on medical imaging*, 41(3): 621–632.

Chen, H.; Qin, Z.; Ding, Y.; Tian, L.; and Qin, Z. 2020. Brain tumor segmentation with deep convolutional symmetric neural network. *Neurocomputing*, 392: 305–313.

Chen, Z.; Du, Y.; Hu, J.; Liu, Y.; Li, G.; Wan, X.; and Chang, T.-H. 2022. Multi-Modal Masked Autoencoders for Medical Vision-and-Language Pre-Training. In *International Conference on Medical Image Computing and Computer-Assisted Intervention*. Springer.

Diao, Y.; Fang, H.; Yu, H.; Li, F.; and Xu, Y. 2025. Multi-modal invariant feature prompt network for brain tumor segmentation with missing modalities. *Neurocomputing*, 616: 128847.

Ding, Y.; Yu, X.; and Yang, Y. 2021. RFNet: Region-aware fusion network for incomplete multi-modal brain tumor segmentation. In *Proceedings of the IEEE/CVF international conference on computer vision*, 3975–3984.

Hamghalam, M.; Frangi, A. F.; Lei, B.; and Simpson, A. L. 2021. Modality completion via gaussian process prior variational autoencoders for multi-modal glioma segmentation. In *International conference on medical image computing and computer-assisted intervention*, 442–452. Springer.

Hinton, G.; Vinyals, O.; and Dean, J. 2015. Distilling the knowledge in a neural network. *arXiv preprint arXiv:1503.02531*.

Hu, M.; Maillard, M.; Zhang, Y.; Ciceri, T.; La Barbera, G.; Bloch, I.; and Gori, P. 2020. Knowledge distillation from multi-modal to mono-modal segmentation networks. In *International Conference on Medical Image Computing and Computer-Assisted Intervention*, 772–781. Springer.

Jia, Q.; and Shu, H. 2021. Bitr-unet: a cnn-transformer combined network for mri brain tumor segmentation. In *International MICCAI brainlesion workshop*, 3–14. Springer.

Karimijafarbigloo, S.; Azad, R.; Kazerouni, A.; Ebadollahi, S.; and Merhof, D. 2024. Mmcformer: Missing modality compensation transformer for brain tumor segmentation. In *Medical imaging with deep learning*, 1144–1162. PMLR.

Kim, D.; and Kim, T. 2024. Missing modality prediction for unpaired multimodal learning via joint embedding of unimodal models. In *European Conference on Computer Vision*, 171–187. Springer.

Li, S.; Du, C.; Zhao, Y.; Huang, Y.; and Zhao, H. 2023. What makes for robust multi-modal models in the face of missing modalities? *arXiv preprint arXiv:2310.06383*.

Lin, C.-W.; and Chen, Z. 2024. MM-UNet: A novel cross-attention mechanism between modules and scales for brain tumor segmentation. *Engineering Applications of Artificial Intelligence*, 133: 108591.

Liu, Y.; Fan, L.; Zhang, C.; Zhou, T.; Xiao, Z.; Geng, L.; and Shen, D. 2021. Incomplete multi-modal representation learning for Alzheimer’s disease diagnosis. *Medical Image Analysis*, 69: 101953.

Ma, F.; Xu, X.; Huang, S.-L.; and Zhang, L. 2021. Maximum likelihood estimation for multimodal learning with missing modality. *arXiv preprint arXiv:2108.10513*.

Mordacq, J.; Milecki, L.; Vakalopoulou, M.; Oudot, S.; and Kalogeiton, V. 2024. ADAPT: multimodal learning for detecting physiological changes under missing modalities. *arXiv preprint arXiv:2407.03836*.

Peiris, H.; Hayat, M.; Chen, Z.; Egan, G.; and Harandi, M. 2022. Hybrid window attention based transformer architecture for brain tumor segmentation. In *International MICCAI Brainlesion Workshop*, 173–182. Springer.

Qian, S.; and Wang, C. 2023. COM: Contrastive Masked-attention model for incomplete multimodal learning. *Neural Networks*, 162: 443–455.

Sharma, A.; and Hamarneh, G. 2019. Missing MRI pulse sequence synthesis using multi-modal generative adversarial network. *IEEE transactions on medical imaging*, 39(4): 1170–1183.

Tian, W.; Li, D.; Lv, M.; and Huang, P. 2022. Axial attention convolutional neural network for brain tumor segmentation with multi-modality MRI scans. *Brain sciences*, 13(1): 12.

Wang, H.; Chen, Y.; Ma, C.; Avery, J.; Hull, L.; and Carneiro, G. 2023. Multi-modal learning with missing modality via shared-specific feature modelling. In *Proceedings of the IEEE/CVF Conference on Computer Vision and Pattern Recognition*, 15878–15887.

Wang, P.; Li, Y.; Singh, K. K.; Lu, J.; and Vasconcelos, N. 2021a. Imagine: Image synthesis by image-guided model inversion. In *Proceedings of the IEEE/CVF conference on computer vision and pattern recognition*, 3681–3690.

Wang, W.; Chen, C.; Ding, M.; Yu, H.; Zha, S.; and Li, J. 2021b. Transbts: Multimodal brain tumor segmentation using transformer. In *International conference on medical image computing and computer-assisted intervention*, 109–119. Springer.

Wang, Y.; Zhang, Y.; Liu, Y.; Lin, Z.; Tian, J.; Zhong, C.; Shi, Z.; Fan, J.; and He, Z. 2021c. Acn: Adversarial co-training network for brain tumor segmentation with missing modalities. In *International conference on medical image computing and computer-assisted intervention*, 410–420. Springer.

Wu, R.; Wang, H.; and Chen, H.-T. 2024. A comprehensive survey on deep multimodal learning with missing modality. *arXiv e-prints*, arXiv–2409.

Xing, Z.; Yu, L.; Wan, L.; Han, T.; and Zhu, L. 2022. NestedFormer: Nested modality-aware transformer for brain tumor segmentation. In *International conference on medical image computing and computer-assisted intervention*, 140–150. Springer.

Yao, W.; Yin, K.; Cheung, W. K.; Liu, J.; and Qin, J. 2024. Drfuse: Learning disentangled representation for clinical multi-modal fusion with missing modality and modal inconsistency. In *Proceedings of the AAAI conference on artificial intelligence*, volume 38, 16416–16424.

Yu, B.; Zhou, L.; Wang, L.; Fripp, J.; and Bourgeat, P. 2018. 3D cGAN based cross-modality MR image synthesis for brain tumor segmentation. In *2018 IEEE 15th international symposium on biomedical imaging (ISBI 2018)*, 626–630. IEEE.

Zhang, D.; Huang, G.; Zhang, Q.; Han, J.; Han, J.; and Yu, Y. 2021. Cross-modality deep feature learning for brain tumor segmentation. *Pattern Recognition*, 110: 107562.

Zhang, Y.; He, N.; Yang, J.; Li, Y.; Wei, D.; Huang, Y.; Zhang, Y.; He, Z.; and Zheng, Y. 2022. mmformer: Multimodal medical transformer for incomplete multimodal learning of brain tumor segmentation. In *International conference on medical image computing and computer-assisted intervention*, 107–117. Springer.

Zhang, Z.; Yang, G.; Zhang, Y.; Yue, H.; Liu, A.; Ou, Y.; Gong, J.; and Sun, X. 2024. Tmformer: Token merging transformer for brain tumor segmentation with missing modalities. In *Proceedings of the AAAI Conference on Artificial Intelligence*, volume 38, 7414–7422.

Zhou, C.; Ding, C.; Wang, X.; Lu, Z.; and Tao, D. 2020. One-pass multi-task networks with cross-task guided attention for brain tumor segmentation. *IEEE Transactions on Image Processing*, 29: 4516–4529.

Zhou, T.; Canu, S.; Vera, P.; and Ruan, S. 2021. Feature-enhanced generation and multi-modality fusion based deep neural network for brain tumor segmentation with missing MR modalities. *Neurocomputing*, 466: 102–112.